AUTOMATED CLASSIFICATION OF FLUORESCENT IN SITU CASES BASED ON HER-2/NEU STATUS

F. Raimondo[1], M. A. Gavrielides[1], G. Karayannopoulou[2], I. Kostopoulos[2], K. Lyroudia[3], I. Pitas[1], *Senior Member* IEEE

1. Department of Informatics, Aristotle University of Thessaloniki, 54006 Thessaloniki, Greece. fraimond@aiia.csd.auth.gr, marios.gavrielides@fda.hhs.gov, pitas@aiia.csd.auth.gr,
2. Department of Pathology, Medical School, Aristotle University of Thessaloniki.
3. Department of Endodontology, Dental School, Aristotle University of Thessaloniki. Tel. +30 2310 999627 Fax +30 2310 996304 lyroudia@aiia.csd.auth.gr

ABSTRACT -- The evaluation of fluorescent in situ hybridization images (FISH) is one of the most widely used methods to determine Her-2/neu status of breast samples, a valuable prognostic indicator. Conventional evaluation is a difficult task since it involves manual counting of dots in multiple images. In this paper we present a multistage algorithm for the automated classification of FISH images from breast carcinomas. The algorithm focuses not only on the detection of FISH dots but also on overall case classification. The algorithm includes two combined stages for nuclei and dot detection respectively. The dot detection consists of a top-hat filtering stage followed by 3D template matching to separate real signals from noise. Nuclei segmentation includes a non-linearity correction step, global thresholding and a geometric rule to distinguish between holes within a nucleus and holes between nuclei. Finally, the marked watershed transform is used to segment cell nuclei with markers detected as local h-dome maxima. Combining the two stages allows the measurement of FISH signals ratio per cell nucleus and the collective classification of cases as positive or negative. The system was evaluated with receiver operating characteristic (ROC) analysis and the results were encouraging for the further development of this method.

I. INTRODUCTION

The HER-2/neu (c-erbB2) oncogene is overexpressed in approximately 20-30% of high-grade invasive breast carcinomas. Currently, the two most widely used technologies to determine HER-2/neu status are immunohistochemistry (IHC) and fluorescent *in situ* hybridization (FISH). A recent study by Bartlett et al. [1] recommended screening by immunohistochemistry followed by FISH testing of cases with intermediate staining intensity for the evaluation of Her-2/neu status. The process of evaluating HER-2/neu status from FISH images involves the manual scoring of the ratio of HER-2/neu over CEP 17 dots within each cell nucleus and then averaging the scores for a number of cells in the order of 60. The reading of FISH images is a difficult task since manual dot scoring over a large number of nuclei is a time consuming and fatiguing technique. Several methods have been proposed for the automated evaluation of FISH signals. Most of them focused on automatic spot counting whereas only very few focused on case-based classification of FISH images. Netten et al. [2] focused on automatic counting of dots per cell nucleus in slides of lymphocytes from cultured blood. Their method consisted in selecting regions of interest containing at least one nucleus and in a spot detection using the top hat transform and a nonlinear Laplacian filter. Solorzano et al. [3] developed a method to study leukocytes in blood samples. They segmented nuclei using the ISODATA thresholding algorithm. Then, the watershed algorithm incorporating the distance transform was used to isolate nuclei and FISH dots were detected using the top hat transform. Kozubek et al. [4] developed a system that acquired 2-D and 3-D FISH images. For 2-D analysis, the system segmented the nuclei using bimodal histogram thresholding and morphological features for further binary image processing. Then, the system detected hybridized dots within each segmented nucleus using a watershed-based algorithm. 3-D analysis was performed by analyzing the pre-extracted nuclei and dot features for sequential 2-D slices. Lerner et al. [5-8] proposed a FISH image classification system based on the properties of in- and out-of-focus images captured at different focal planes. In a later study, the authors employed a Bayesian classifier instead of an NN, to avoid dependency on a large number of parameters.

In this paper we present a multistage algorithm for the automated evaluation of HER-2/neu status in breast carcinomas samples. It includes two parallel stages for nuclei and dot detection respectively. It takes into account multiple images of a specific case and quantifies the HER-2/neu status in a collective manner. Moreover, the system is evaluated with ROC analysis in respect to three main tasks: nuclei segmentation, spot detection, and case classification. The paper is organized as follows: Section II describes the database used for the development and evaluation of the method. The method is detailed in section III whereas Section

IV presents the evaluation results and a related discussion. Finally, conclusions are stated in Section V.

II. MATERIALS:

Paraffin sections of 4μm thickness were incubated overnight at 60°C. Deparaffinization, pretreatment, enzyme digestion and fixation of slides were performed using the Vysis Paraffin Pretreatment kit according to the manufacturer's recommended protocol. After proteolysis, tissue sections were denaturated at 85°C for 2 minutes, then the PathVysion HER-2 DNA Probe (LSI HER-2/CEP17 probe, Abbott GmbH and Company, KG, Wiesbaden-Delkenheim, Germany) was added and hybridization took place at 37° C in a moist chamber for 14-18h (overnight incubation). The following day the slides were washed with post-hybridization buffer (2X SSC and 0,3% NP-40) at 72°C for 2 minutes, followed by counterstaining of the nuclei with 4, 6-diamino-2phenylindole dihydrochloride (DAPI). For each specimen, at least 60 non overlapping nuclei were scored for both Her-2/neu and chromosome 17 signals by image analysis. Hybridization signals were enumerated utilizing a Zeiss, Axioskop 2 HBO 100. Her-2/neu gene amplification was determined by a ratio of Her-2/neu gene copies to chromosome 17 centromeres. According to the manufacturer's recommendations the cases with a ratio ≥2 were determined as amplified, while those having a ratio <2 as not amplified.

III. METHOD:

The algorithm for the classification of FISH images was based on the accurate measurement of red/green spot ratio (corresponding to the ratio of HER2/CEP 17) per cell nucleus. For that reason, two parallel stages for spot detection and cell nuclei segmentation were developed as described below.

A. FISH SPOT DETECTION

Due to the presence of noisy areas consisting of large stains, a top-hat filtering was first applied on FISH image red and green channels for noise removal. As the typical grey level histogram of the top-hat output presents a strong unimodal trend a modification of the algorithm proposed in [9] was used to estimate two binary thresholds. For this application, we did not apply the method on the entire image, but rather on the pixels belonging to the last k bins of the histogram. If we indicate with N the total number of pixels of the image and with $h(i_n)$ the intensity image histogram value relative to the $n-th$ bin, then k is the minimum integer such that:

$$\sum_{n=N-k}^{N} h(i_n) \geq N \cdot p \qquad (1)$$

The value of p was chosen equal to 2.5%. Then we use normalized cross correlation to measure the similarity between every candidate spot and two spot templates, one to compare with candidate from red channel and the other for the ones from green channel. The two spot templates windows T_G and T_R are estimated by averaging the respective spot channel intensities:

$$T_R(x,y)=\frac{1}{N_R}\sum_{i=1}^{N_R} f_{R_i}(x,y) \qquad T_G(x,y)=\frac{1}{N_G}\sum_{i=1}^{N_G} f_{G_i}(x,y) \qquad (2)$$

Where N_R and N_G are the number of used red and green spots identified from an expert in a training set, $x=1,...,7$ and $y=1,...,7$ are coordinates in a 7×7 window positioned on every spot center, f_{R_i} and f_{G_i} are the red and green channel intensities of $i-th$ spot image. The two resulting images C_R and C_G, are multiplied for two binary masks, one obtained from the thresholding of the top-hat output and the other from the nuclei segmentation. In order to select red/green spot positions, two positive thresholds Th_R and Th_G are used; spots with a value of C_R and C_G lower then Th_R and Th_G respectively, are discarded while the remaining ones are used as input for the next selection step of the FISH spot detection algorithm.

Finally**,** for every detected spot from the previous step, a channel intensity contrast C_M measure is performed as:

$$C_M = \frac{\left\| \boldsymbol{v}_{for} - v_{back} \right\|}{\left\| v_{back} \right\|} > T_{CM} \qquad (3)$$

Each of the three components of the vector $\boldsymbol{v}_{for}$ is estimated considering the average red, green and blue channel intensity of the pixels of a 5×5 window positioned on every spot center, while each of the three components of vector $\boldsymbol{v}_{back}$ is estimated considering the average red, green and blue channel intensity of the pixels surrounding the previous window. The thresholds Th_R, Th_G and T_{CM} are empirically chosen in order to minimize spot classification error over the FISH images used for training.

B. CELL SEGMENTATION

Cell nuclei segmentation is performed on the FISH image blue channel. A nonlinearity correction step incorporating the square root function is applied in order to reduce the unbalanced channel intensity present in the cell nuclei body. The algorithm by Otsu et al [10] was employed to determine

the threshold for initial nuclei segmentation. The binary image resulting from thresholding sometimes contains holes even in a single nucleus body region. This kind of holes has to be filled to enable correct nuclei segmentation. On the contrary, holes present in inter nuclei zones of overlapping nuclei should not be filled. The two types of holes are illustrated in Figs 1a and b respectively. A geometric approach is employed to distinguish between these two types of holes. Let *P* be the percentage of the perimeter pixels of a circle of radius *R* centered around a hole centroid that are contained in the nucleus region. It can be observed from Fig. 6, that the value of *P* is much higher for the first type of hole (inter nuclei) than the second type of hole (nucleus region). The chosen value of the radius *R* is 60, that is slightly bigger than the average nuclei radius.

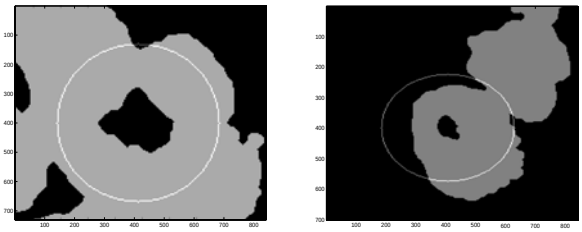

a) b)

Fig.1: a) Hole due to overlapping nuclei (inter nuclei case); b) Nucleus body hole.

It was found experimentally that the value for *P* varied in the range of 90% to 40% for holes of the first type and second type respectively. Finally the marked watershed transform [11], using as markers the local maxima of the distance transform, is applied. The distance transform [12] is applied to the binary image obtained from the previous step. In order to reduce spurious local maxima we calculate *h-domes* of resulting image [13]. We can define the *h-dome* as a region of pixels wherein every pixel has an intensity value greater than any of the pixels surrounding the region and the maximum intensity difference between two pixels in the region is smaller than or equal to *h*. Characteristic values of *h* are in the range $[0.5 : 2]$. Nuclei touching the image border are removed from the final segmented image because they are not considered in the spots per cell counting. The results of the spot detection and nuclei segmentation steps were combined and the ratio of red/green spots per nucleus was calculated as will be described in the next section.

IV. RESULT/DISCUSSION

The algorithm was evaluated with respect to three different tasks: spot detection, cell nuclei segmentation and case-based classification as will be described below.

In order to estimate the performance of the algorithm for detecting FISH spots, a testing set of 40 FISH images was used. The true location of 887 red spots and 751 green spots was labeled by an expert. The same expert identified the location of 385 true red spots and 334 true green spots in 18 different FISH images that were employed as training set to estimate spot shape templates. ROC curves were constructed by collecting pairs of sensitivity (or true positive rate) and false positive rate by varying the threshold applied to top-hat output. Curves were estimated for red and green spots separately and are displayed in Fig. 2.

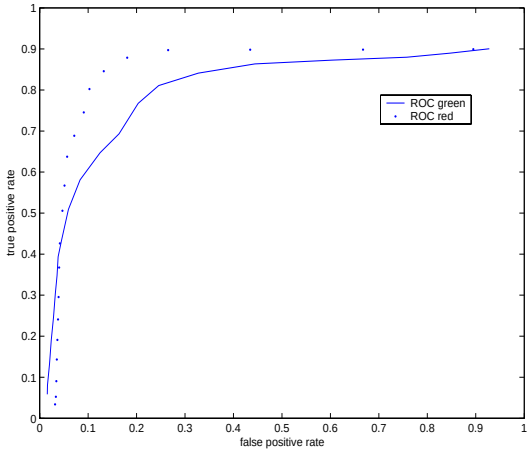

Fig.2: ROC curves relative to red and green spots detection.

As a demonstration point, the algorithm can reach a sensitivity of about 92% and 80% for red and green spots respectively at a false positive rate of about 25%.

In order to evaluate the performance of the algorithm for cell nuclei segmentation, the ratio between the area of intersection of segmented nucleus with true nucleus region over the area of the union of two regions was calculated. The ground truth for the correct nucleus boundaries was determined from an expert manually. ROC curves were constructed by varying a threshold for the ratio of intersection over union. Fig.3 shows the resulting ROC curves for three values of *h* {0.5, 1.0, 1.5}.

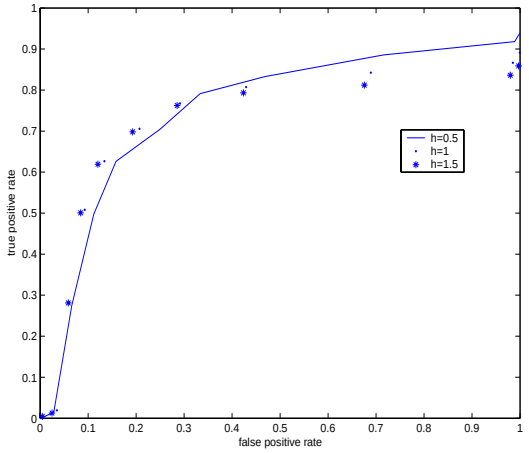

Fig.3: ROC curves relative to the cell nuclei segmentation.

As we can see performances are not much sensitive to the value of *h*. It has to be noted here that for this application it is more crucial to not discard a true nucleus than to avoid

merging overlapping nuclei since dot counting per nucleus is averaged and it is not overly sensitive to two nuclei being counted as one.

Twelve patient cases, six of which were previously classified by an expert as positive and six that were classified as negative, were employed to evaluate the precision of the algorithm in classifying the different cases. For every segmented nucleus where at least one red spot was present the ratio d between the number of red and green spots was calculated. In the case that the number of green spots is zero, we set the number green spots equal to one. For each case the histogram of d was calculated in order to estimate the probability $P(d \geq 2)$ of having a ratio red/green greater or equal then two. The values of $P(d \geq 2)$ for each of the testing cases were given in Tab. 1.

Table 1. Values for the estimation of the probability to have a ratio greater or equal to 2 for each of the testing cases.

Pos. 1	Pos. 2	Pos. 3	Pos. 4	Pos. 5	Pos. 6
0.531	0.663	0.525	0.488	0.515	0.538
Neg. 1	Neg. 2	Neg. 3	Neg. 4	Neg. 5	Neg. 6
0.239	0.319	0.287	0.201	0.323	0.245

It can be seen from Table I that all cases can be correctly classified as either positive or negative (100% sensitivity with 0 false positives) by using a proper threshold for the statistic $P(d \geq 2)$. These preliminary results show that a fully automated method can accurately distinguish between normal and abnormal breast tissue samples. A larger database of FISH images of breast tissue is being prepared in order to examine how well these results can generalize in a broader population.

V. CONCLUSION

We have developed a method for the automated evaluation of Her-2/status in breast samples by FISH image analysis. The method uses two parallel multistage algorithms, the first one for the detection of the red and the green spots and the second one for the cell nuclei segmentation. The outputs of the two algorithms were merged for estimating the average red/green ratio per cell nucleus. The performance of the proposed method was evaluated using ROC curves both for the detection of the red and the green spots and for the cell nuclei segmentation. Moreover, the overall algorithm performance for case-based classification of FISH images showed the ability of the system to distinguish between positive and negative cases. The evaluation results were encouraging for the further development and evaluation of this method.

ACKNOWLEDGEMENT

This work was supported by the EU project Biopattern: Computational Intelligence for biopattern analysis in Support of eHealthcare, Network of Excellence Project No. 508803.

REFERENCES

[1] J. Bartlett, E. Mallon, and T. Cooke, “The clinical evaluation of Her-2 status: which test to use?”, *Journal of Pathology*, vol. 199(4), pp. 411-417, 2003.

[2] H. Netten, I. T. Young, L. J. van Vliet, H. J. Tanke, H. Vroljik, and W. C.R. Sloos, "FISH and Chips: Automation of fluorescent dot counting in interphase cell nuclei". Cytometry, vol. 28(1), pp. 1-10, 1997.

[3] C. O. de Solorzano, A. Santos, I. Vallcorba, J-M Garcia-Sagredo, and F. del Pozo, "Automated FISH spot counting in interphase nuclei: Statistical validation and data correction", *Cytometry*, vol. 31(2), pp. 93-99, 1998.

[4] M. Kozubek, S. Kozubek, E. Lukasova, A. Mareckova, et. al., "High-resolution cytometry of FISH dots in interphase nucleus nuclei", Cytometry, vol. 36(4), pp. 279-293, 1999.

[5] B. Lerner, W. F. Clocksin, S. Dhanjal, M. A. Hulten, C. M. Bishop, "Feature representation and signal classification in fluorescence in-situ hybridization image analysis", *IEEE Transactions on Systems, Man, and Cybernetics*, Part A 31(6), 655-665, 2001.

[6] B. Lerner, "Bayesian fluorescence in situ hybridisation signal classification", *Artificial Intelligence in Medicine*, 30(3): 301-316, 2004.

[7] B. Lerner, W. F. Clocksin, S. Dhanjal, M. A. Hulten, and Christopher M. Bishop, "Automatic signal classification in fluorescence in-situ hybridization images, *Bioimaging,* vol. 43(2), pp. 87-93, 2001.

[8] W. F. Clocksin and B. Lerner, "Automatic Analysis of Fluorescence In-Situ Hybridisation Images", BMVC 2000.

[9] P.L. Rosin, "Unimodal thresholding", *Pattern Recognition*, vol. 34(11), pp. 2083-2096, 2001.

[10] N. Otsu, “A thresholding selection method from graylevel histogram”, *IEEE Trans. on Systems, Man and Cybernetics*, 9 (1):62–66, 1979.

[11] S. Beucher, and F. Meyer, “The morphological approach to segmentation: the watershed transformation”, in E.R. Doughterty (Ed.), *Mathematical morphology in image processing*, (New-York: Dekker, 1992).

[12] Pratt, William K., *Digital Image Processing*, New York, John Wiley & Sons, Inc., 1991.

[13] L.Vincent,”Morphological grayscale reconstruction in image analysis: Applications and efficient algorithms”, *IEEE Trans. Image Processing*, vol. 2(2)**,** 176-201, 1993.